Minimum Extraction of Sub-ROI for Near-Lossless Compression on Medical DICOM Image

Ghalib Salman
Department of Artificial Intelligence Techniques, Middle Technical University, Iraq
dr.ghalib@mtu.edu.iq

Arif Arif
Department of Computer Systems Techniques, Middle Technical University, Iraq
dr.arifsameh2016@mtu.edu.iq

*Sarina Mansor
Faculty of Artificial Intelligence and Engineering, Multimedia University, Malaysia
sarina.mansor@mmu.edu.my
Corresponding Author

Abstract: *Medical image compression recorded increasing importance over recent decades due to the widely adoption of Tele-Medicine application. Besides the non-ignorable size of produced medical images, some Medical Imaging Devices (MID) such as Digital Imaging and Communication in Medicine (DICOM) produce serial of medical images for each single patient. In other words, to tele-diagnose a patient case, the whole series of images must be transmitted, which causes a huge total size of image. Generally, all types of serial-type medical images contain correlated images due to their similarity of image details. In DICOM images, there are three major parts of each image, non-related parts generated by the imaging device, Region of Interest (ROI), and sub ROI. The main idea of this paper consists of two concepts, firstly to focus on the correlation between successive images to find the differences between them increasing the Compression Performance (CP). The second concept focuses on the sub ROI in lossless compression to preserve the medical details and compressing other parts with lossy methods under acceptable level of Peak Signal to Noise Ratio (PSNR). This provides higher CP and without corrupting sensitive details. Due to similarity between successive images, they are subtracted to produce large serial of zeros within corresponding similar parts and other differences within other areas. Depending on long series of zeros produced in subtraction process, this work adopted Run Length Encoding (RLE) to compress image-subtraction result. The compressed form RLE is re-compressed using Arithmetic Coding Technique (ACT) as an effective compression method. The order of combining RLE & ACT is significant due to the nature of compressed data. The proposed compression scheme recorded superior performance (cp=55.7) as benchmarking with other published works in medical image compression field, where it records (1.1) as an enhancement from the nearest performance. This performance is under the best circumstances, where the highest performance in some circumstances was where cp=59.4.*

Keywords: *Medical image compression, Sub-ROI, near-lossless compression, DICOM Images, coding techniques.*

Received April 29, 2025; accepted December 18, 2025
https://doi.org/10.34028/iajit/23/4/14

1. Introduction

Using image compression techniques with medical images is mandatory in order to increase the efficiency of Tele-medicine applications. On the other side, some medical imaging techniques produces series of images for each case, which produces higher demand for storage space, and more required time for image transmission [15]. Different applications and approaches were adopted and applied to compress Digital Imaging and Communication in Medicine (DICOM) images. Different works focused on different aspects of medical image to achieve higher Compression Performance (CP) such as focusing on Region of Interest (ROI) areas, using coding techniques, depending on image transforms, or differences between successive images [1, 2]. DICOM imaging technique produces set of serial images for each case (patient), where the patient swallows a specific liquid (Barium Liquid) supervised by the technician. Then, the suspected area of patient body to be infected is captured to monitor the liquid motion. Technicians and doctors have the liquid shape, in each image, as a basis for diagnosis process [3, 4].

Due to liquid motion along Esophagus and Pharynx parts, liquid takes different shapes and lengths. In other word, liquid changeability indicates infected areas, where the liquid draws unusual shapes initially recognized by technicians and doctors. Each DICOM image is divided into three major parts as in Figure 1, non-related areas, ROI area (patient image part), and sub-ROI (liquid shape area). Figure 1 illustrated the non-related part as the white circle inside the black square, which do not contain any medical information related to the patient. The ROI area is highlighted with red rectangular containing the captured part form patient body. The most important part is the sub-ROI (inside the blue oval), which indicate liquid attributes (location, shape and motion). The sub-ROI is the cornerstone of diagnosis [5] and rest of ROI area is significantly less important in diagnosis process. Where DICOM images are successively captured for the same patient, sub-ROI area is changeable due to liquid motion, and all other parts of ROI are almost identical.

This paper utilized these attributes to build the proposed compression framework. It depends on subtracting the successive images after extracting the smallest ellipse-shape contains the sub-ROI to be compressed using lossless compression technique. The rest of ROI area is compressed using lossy compression technique, while irrelative parts are ignored. The rest this paper is organized as follows: Previous Work section reviews related works published in DICOM medical image compression field. Methodology section discusses the related aspects of built compression framework. Results and Discussion section discusses and evaluate yielded results. Conclusion section lists the concluded remarks form building this compression framework.

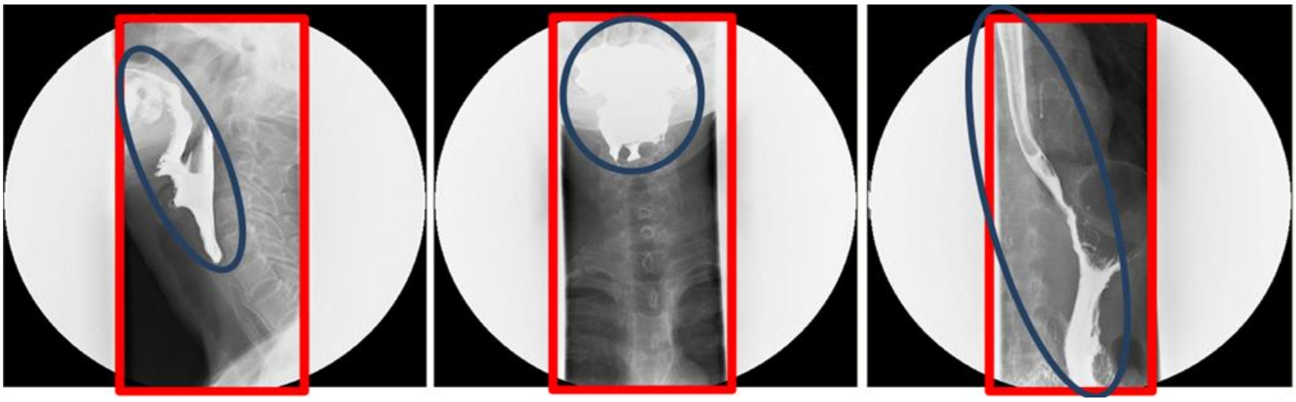

Figure 1. DICOM images contain three principal parts, non-related (Black square and white circle), ROI (Red rectangle), and sub-ROI (Blue Oval) parts.

2. Previous Works

Due to the importance of interior details, many proposed works depended on lossless compression techniques to preserve such details [7, 9, 25]. Such works and methodologies usually yield low performance of compression to preserve important details. On the other side, such techniques produce a high-size compressed -image, which degrades the performance of tele medicine applications besides requiring high space for their storage. Dhar *et al*. [10] discussed applying lossless and lossy compression to review the differences yet, the authors yielded considerable .between them performance of compression with low level ofPeak Signal to Noise Ratio (PSNR).Other works applied lossy compression techniques with acceptable PSNR [11] ratio to handle medical image compression depending on extracting ROI area. Extracting ROI areas raises their compression performance to about (49) for Compression Ratio (CP). Other set of authors combines between Discrete Wavelet Transform and Run Length Encoding (RLE) techniques to compress serial images, yet the adopted compressing the whole ROI area without focusing on liquid motion areasthey ,In addition . workedon multiple images for the same patient captured for higher image quality rather than considering patient progress [6]. Due to insufficient performance for ROI compression, some authors combined more than one compression technique to enhance their proposed scheme for medical image compression [13]. They handled and focused on the entire ROI since their images do not contain liquid motion. Despite they adopted near-lossless compression scheme, their results didn't record significant differences form previously published ones.

As an analysis, previous works handled serial medical images in different ways. Some of them tended to focus on ROI area, while others preferred to combine multiple compression techniques. On the other side, some authors preferred to preserve sensitive medical information using lossless compression techniques, while others preferred to increase CP measure using lossy techniques. Despite the considerable yielded results, the best of our search didn't find medical image compression that depends on sub-ROI area considering ROI area as a reference.

3. Methodology

3.1. Digital Imaging and Communication in Medicine

DICOM is a type of Medical Imaging Devices (MID) that produces series of successive medical images for the same patient inspection [14], where each image represents a stage of inspection process [16, 29]. One of the most popular types of DICOM image is Fluoroscopy, which produces a serial of X-ray images using gray scale coloring system. The major technique of Fluoroscopy depends on the swallowing process, which has oral, pharyngeal, and Esophagus stages [17]. Sometimes, the oral stage is sub-classified as two further sub-types oral-propulsive and oral-preparatory, which involve together solid-food into a swallow-ready propulsion and consistency to be received by Pharynx [18]. Next, within pharyngeal stage set of valves are closed generating a system of pressure preventing reverse flow of the contents back into the nose. Within the final stage, the upper sphincter is relaxing to allow aforementioned bolus to get into the Esophagus. Along the swallowing process, different clinical signs are noticed, where the technician must be aware about them. These signs construct the skeleton of the medical opinion should be built [19]. The medical indications of infection differ due to swallowing stage, shape of swallowed liquid inside the infected organ, coughing and possible indication of material aspiration [20]. One of the most standard of swallowed liquid is the swallowed Barium, which provides dynamic inspection of DICOM x-ray images [21].

As a summary, the aforementioned information indicates the high importance of path, shape, and stages of swallowed liquid. In other words, medical inspection depends on sub-ROI areas rather than the total ROI and other related areas.

3.1.1. Paper Scope and Adopted Dataset

different human organs, DICOM devices provide different forms of medical images such as gray-scale and colored X-ray. In some cases, DICOM devices produce the inspection results in a compressed video form like (MPEG) [7, 8, 19]. The most popular form among them is the produced serial of images by Fluoroscopy devise for Pharynx and Esophagus, which is adopted in this work. This type of DICOM images (gray-scale X-ray) is adopted in this work due to its significantly large production overall the world by hospitals and medical centers [17, 18]. Besides, Fluoroscopy image are freely available within different standard datasets [22, 23]. This work conducts its experiments using the DICOM-image dataset that contains over 960 images for Pharynx, Esophagus, and different other human organs [24].

3.2. ROI Extraction

This step has two major concerns, ignoring non-related, and focusing on the minimum ROI area. The non-related areas are represented by the outer Black Square and white circle, where ignoring them extracts the middle rectangle contains the whole medical information as aforementioned. Such process avoids handling redundant areas with high amount of irrelevant data. Where they have no medial information, they will be deleted at the compression stage and compensated As Figure 2 explains, the white circle inside black square is generated and merged with the decompressed ROI to construct the restored DICOM image.

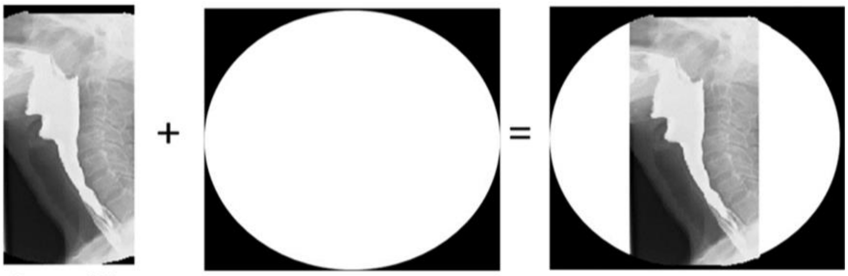

Decompressed ROI. Generated non-relative parts. Restored Image.

Figure 2. Ignoring non-relative image parts during compression stage and re-generating them at the decompression stage.

As in Figure 3, the standard cropping algorithm [26], adopted in this work, ensures including all ROI-area details even if some of non-related details are included. This is to ensure avoiding the loss of any of ROI details. It's noticeable that all medical information that constructs the basis of diagnosis concentrated along the

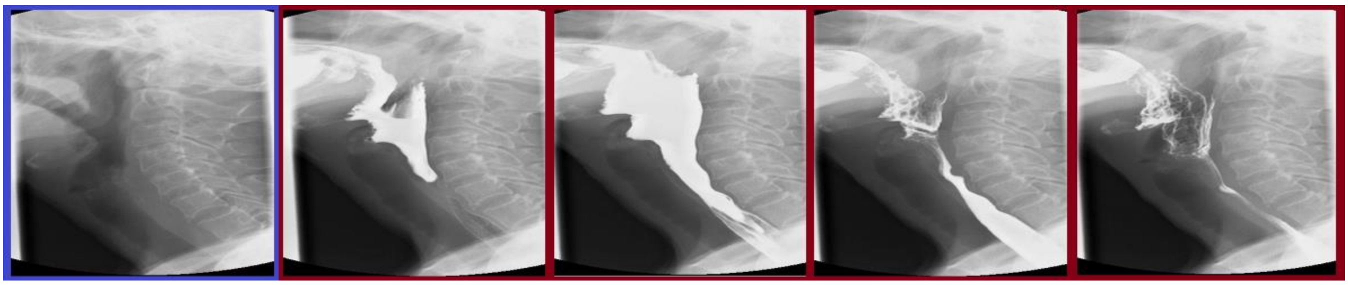

a) Reference image. b) Different stages of swallowing liquid.

Figure 3. A sample of series of DICOM images, where first one is a reference image without swallowing liquid.

liquid path. Thus, this work proposes finding the smallest ellipse that contains all points of liquid motion inside the image even if the cropped sub-ROI area contains points from outside the liquid-motion area, which ensures cropping all of sub-ROI points. Since most of cropped ellipse types are rotated slightly to left, this work adopts the standard equation of ellipse that considers rotation issues [27]:

$$\frac{(x\cos(\theta)+y\sin(\theta))^2}{a^2}+\frac{(x\sin(\theta)+y\cos(\theta))^2}{b^2}=1 \tag{1}$$

The vertical (y1-y2) and horizontal (x1-x2) differences are used to compute cos(θ) & sin(θ) values.

Assume that yo=y1-y2, and xo= x1-x2 then [27]:

$$r_o=\sqrt{y_o^2+x_o^2} \tag{2}$$

$$cos\ cos\ (\theta)\ =\frac{x_o}{r_o} \tag{3}$$

$$sin\ sin\ (\theta)\ =\frac{y_o}{r_o} \tag{4}$$

While Figure 4-(a explains compressing the first image in the DICOM series of images (reference images), Figure 4-(b explains the followed steps in compressing second to last image in whole series of DICOM images, which consists of the following major steps:

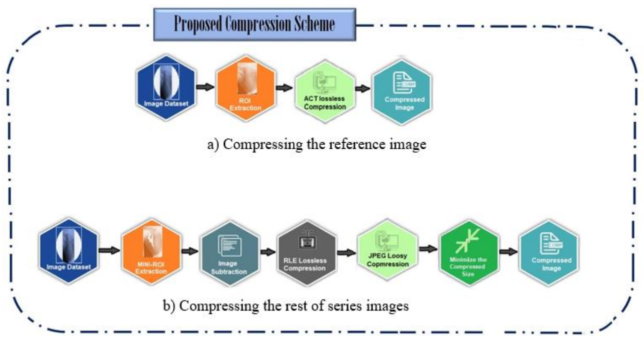

Figure 4. The general diagram for the compression.

On the other side, next pseudo code explains algorithmic steps of extracting process for the ellipse contains minimum possible sub-ROI. In order to ensure restoring the cropped ellipse into the right place, four points are stored as a meta-data for compressed images (A1, A2, B1, and B2). These points are used re-build the ellipse equation, which indicates the original place of the decompressed image points. Each restored sub-ROI is applied on the reference image of DICOM series of images. Determining the cropped ellipse ensures cropping the minimum sub ROI, and the rest of ROI is compensated from the reference image. Such determination is easily found out depending on (A1, A2, B1, and B2) points, which are efficiently determined after using an efficient standard segmentation algorithm [28]. The major role of segmentation step is to determine these points, which are used to crop sub-ROI from the original ROI. Figure 5 illustrates ellipse determination steps.

3.3. Image Subtraction

In this step, this work depends on compressing the difference between two successive images rather than compressing a single image itself. Subtracting the successive image provide considerable amount of successive values (zeros) for the corresponding similar-detail areas [30]. In such case, using RLE technique provides considerable performance [31], and RLE result is re-compressed using the standard Arithmetic Coding Technique (ACT) algorithm. Adopting ACT is because applying RLE produces set of values with different frequencies (probabilities), which enhances the CP of ACT algorithm [29, 31]. Expected results of subtraction are either zeros for the corresponding details, or significant differences within areas that contain different corresponding details. Yet, due to some of imaging errors, it was noticed that some differences record trivial values (close to zero), which indicates close levels of pixel values in corresponding areas. Such differences indicate imaging errors rather than liquid motion, value differences of liquid motion are represented by value transfer from dark area (low-level values), which is the original color level, to the illuminated area (high-level values) representing liquid area [5, 8]. Ignoring such trivial differences and set them to zero does not change liquid area since there is no differences from low to high levels of values or vice versa. To ensure that, acceptable levels of PSNR determine the quality of decompressed images.

Pseudo code (1): major steps for extracting the minimum ROI

Scan the image highest A1(x1, y1), lowest one A2(x2, y2), most right B1(x3, y3) and B2(x4, y4) points of the liquid-motion area.

Use these points as the major {A1& A2} and the minor {B1& B2} vertices

Use A1- A2 and B1- B2 distances to be the lengths of long and short diameters.

Depend on diameters and vertices to build the required ellipse.

Scan the image to determine liquid point outside the ellipse (if any)

Adjust the vertices A1, A2, B1 and B2 in addition to diameters A1-A2 and B1- B2 such that the required ellipse will contain all liquid points.

Crop the ellipse by assigning image points:

$$Pi(x_i, y_i) = \{Pi(x_i, y_i)\ if\ the\ point\ inside\ the\ ellipse\ 0\ Other\ wise\}$$

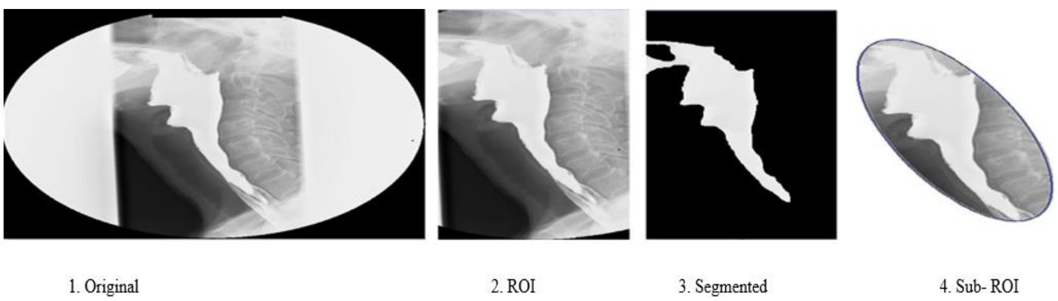

Figure 5. Steps of extracting ROI and segmenting it to determine the sub-ROI.

3.4. Minimizing The Compressed Size

This work adopts an extra compression technique that minimizes compressed-image size and maximizes the CP level. It simply doubles CP value by shrinking the size of the compressed image by 50%. The major concept depends on bit/ byte concepts using standard

Mean Normalization Equation (NME) [32], which converts any range of values into the new required range as in Equation (5). This equation is the standard form of normalization, which subtracts the minimum value (min) within the original range from each value xi. Subtraction result is divided by the difference between the maximum value of the original range and min values. This division converts any range of values into (0- 1) range, which can be converted to any new range (b-a). In sometimes it's desired to start the new set of values from starting value (c).

$$x_o = \frac{x_i - min}{max - min}(b - a) + c \quad (5)$$

In this work, the original set of values have minimum value (0) and maximum value (255), where each of them is represented using a single byte (8 bits). The new range (b-a), in this work, is (16) that are represented using 4 bits only. Representing the original values using 4-bit values enables each two values to be represented using a single byte. Next example is a numerical explanation for this proposed compression method, where it contains for arbitrary number taken from a DICOM image. The first line (Original) represents the original numbers in the Decimal form of (0- 255) range, where the second line (8 Bits) represents the same numbers in a byte form of binary numbering system.

By applying Equation (5) on each original number to convert it into (0-15) range as in Equation (6), the new numbers are represented in the next line (Compressed) shows that (Compressed) line numbers can be represented using only 4 bits

Original	22	92	153	99
8 Bits	00010110	01011100	10011001	0110011

$$x_o = \frac{x_i - 0}{255} \quad (6)$$

Compressed	0	8	15	9
4 Bits	0000	1000	1111	1001

By concatenating each two successive (4 Bits) numbers, a single byte of 8 bits is produced in (Combined) line, and the line (Results) represents final numbers in Decimal numbers.

Combined	00001000	11111001
Results	8	249

As a result, the four numbers 22, 92, 153, and 99 are converted in two numbers 8 and 249. Accordingly, the final number of values has half of number of values taken from the compressed image. And as a real example, one of the compressed images had (26815) bytes as size, which was further compressed into (13408) bytes. Producing half size of the compressed image doubles CP value. This can be explained using the mathematical formula of CP, which is the Original File Size (OFS) divided by the Compressed File Size (CFS) [33] as in Equation (7):

$$cp = \frac{OFS}{CFS} \quad (7)$$

And due to Equation (8), where the compressed size is further compressed in the half then

$$new\ cp = \frac{OFS}{\frac{1}{2}CFS} = 2 \times \frac{OFS}{CFS} = 2 \times CP \quad (8)$$

At the decompression stage, decompressed values are re-converted into (0-255) range regardless their original range. This ensures accomplishing Histogram Equalization to the original image, and if the original DICOM image to be compressed is dark or illuminated, the restored image is enhanced. PSNR values determine if the quality of restored image is distorted or acceptable, which means that this operation combines between compression and image enhancement.

4. Results and Discussion

The experiments of this work are performed using computer specifications (software and hardware) illustrated in Table 1. The proposed compression scheme was applied on 960 DICOM images captured from different views, and each of them is a gray-scale image of 512×512-pixel size. To evaluate the yielded results, two measures were used in this work, Peak Signal to Noise Ratio (PSNR) for acceptance of decompressed image and CP to gauge the compression performance.

Table 1. Machine specifications used to carry out experimental results.

Computer Components	Details
CPU	Intel Core i7-10750H CPU @ 2.60 GHz (12 CPUs)
Internal RAM	32 GB
GPU	RTX 2070 of 8 GB with 2304 CUDA cores
Programming Language	Python 3.7
Operating System	Windows 10 64-bit

This work adopted two standard compression techniques RLE and ACT due to nature of handled data. RLE is adopted to compress the result numbers of successive image subtraction, where such images contain long sets of connected series of zeros. Since applying RLE produces set of numbers with specific frequencies (probability) and ACT depends on value probabilities [33], ACT is adopted to compress the result compressed images from RLE. It's obvious that adopting RLE and ACT is due to the nature of numbers to be compressed, which means that both of them should be adopted with preserving the same order. Table 2 summarizes yielded results from applying RLE, ACT, and their combination. Experimental results shows that apply each of them alone recorded significantly less performance than their combination. On the other side, applying ACT recoded better performance than RLE, and this is justified due to concepts of both of them. RLE has the privilege of compressing similar successive values, which is not always available. On the other hand ACT depends on values occurrence but not necessarily successively, where it depends on their probability. Accordingly, the sequence RLE then ACT than the opposite since RLE utilizes considerable amount of successive values. On the contrary, applying ACT firstly distort the successively values degrading the performance of RLE.

Table 2. Yielded CP values for applying RLE, ACT and their order.

Compression Method	CP
RLE only	9.1
ACT only	11.7
RLE then ACT	55.7
ACT then RLE	29.8

This work adopted extracting minimum possible area contains the medical information, which can be used in building the medical diagnosis. Selecting sub-ROI rather than the whole ROI produced significant enhancements in compression performance, yet compressing only parts of ROI and ignoring the rest parts may degrade restored-image quality. PSNR is adopted in most of (lossy and near-lossless) image compression researches to evaluated decompressed images [1, 10, 34]. It is essentially defined as the ratio of maximum signal power normalized by corrupting-noise power, which can affect the representation fidelity. Since plenty of signal types are represented within wide ranges, many literatures express PSNR is usually expressed as a logarithmic quantity using the decibel scale [12, 35]. Table 3 summarizes the average results yielded from compressing the entire original image, the ROI area after excluding non-relative areas, and finally the sub-ROI by selecting only liquid-motion areas. It was noticed that PSNR recorded high values for all types, which indicates the high quality of restored image in all types. Yet CP recorded different levels of performance, where compressing the whole image recorded significantly weak performance regarding the others. Compressing only ROI area yielded encouraging enhancement, but the best performance was yielded by compressing sub-ROI areas.

Table 3. CP and PSNR values over the whole image, ROI and sub-ROI.

Compression Method	CP	PSNR
The whole image	3.4	67.15
ROI	22.7	62.07
Sub-ROI	55.7	61.92

Since the subtraction of successive images creates considerable amount of linked lists of continuous zeros, RLE has suitable role to compress such data. In addition, using ACT to compress the results of RLE compression enhances the CP performance. As a result, compressing the stand alone images without subtraction didn’t record worthy results to be mentioned.

Subtracting the successive images creates zero values for subtracting similar corresponding areas, and recorded significantly high differences for the areas contain moving form black to white areas and vice versa. In some cases trivial differences were recorded, which were small to represent transferring between white and black area. Such differences are justified as imaging errors indicating subtracting similar areas with slight differences occurred because of imaging errors. These differences are ignored to be considered as zeros, where they’re expected to be from subtracting similar areas. Maximum difference of such type was recorded as 5 and less. Table 4 illustrates the effects of ignoring trivial differences on CP and PSNR levels. Ignoring differences up to (2) recorded high quality of restored images (PSNR) and high levels of Compression Performance (CP). Ignoring differences equal to (3) recorded unstable performance of compression and PSNR. Ignoring differences equal to (4 and 5) recorded significantly high levels of CP measure indicating considerable performance of compression. Against that, PSNR recorded significantly low levels indicating degraded quality of restored images. Considering aforementioned results, this work proposes ignoring no more (2) level of trivial differences to preserve restored-image quality.

Table 4. The effects of ignoring different levels of trivial differences.

Level of ignored trivial values	CP	PSNR
1	44.8	63.02
2	55.7	62.07
3	Instable	
4	57.1	33.7
5	59.4	15.11

As aforementioned, the average performance of CP was 55.7, yet this proposed compression scheme, in some cases of sub-ROI significantly small, recorded the best performance reaching 66.4.

Table 5. Benchmarking with State of Art literatures in medical image compression.

Literature	CP	PSNR
Viswanthan and Kalavathi [37]	5.9	50.71
Shyamala and Geetha [31]	11.8	50.71
Zafar *et al*. [39]	33.5	59.34
[37] Kalavathi and Viswanthan	54.6	44.91
Our proposed scheme	55.7	62.07

As benchmarking with State of Art literatures, this work recorded superior results regarding CP and PSNR. Table 5 shows the benchmarking results with different published documents. Viswanthan and Palanisamy [37] adopted the standard Wavelet transform for medical image compression without using pre-processing operation as in our work. As a result, their results were the lowest performance in the comparison. Other set of authors enhanced their work by combining two standard transforms ACT and Discrete Cosine Transform (DCT). Using YCbCr coloring system, the authors applied their adapted version of DCT combined by the standard version of ACT [38]. Zafar *et al.*, [39] adopted a local adaptive predictor depending on block-based method to compress DICOM images utilizing neighborhood concept. Their work suffered from pre-processing process that make the handled data suitable for the compression technique. Zhao *et al*., [40] were the nearest performance-based compression algorithm to our proposed compression scheme regarding cp value. Yielded values of PSNR shows that their restored image recorded high effectiveness.

5. Conclusions

Medical images were fused, combined [36], and compressed for sensitive applications when the performance must balance between compression performance and preserving the sensitive details. This paper proposes a near-lossless compression scheme, which preserves the important medical details and ignores the non-relative information that does not participate in the medical diagnosis. Such approach increases compression performance without affecting important details. The major concept of the proposed scheme depends on ignoring the non-relative image area to extract ROI areas and then extracting the minimum possible sub-ROI areas to be compressed. Then the scheme tends to compressing the differences between successive images rather than compressing the image itself. Such approach produces relatively large sets of zeros in subtracting the similar corresponding areas, which makes the media suitable to be compressed by the standard RLE algorithm. The results of RLE are compressed using the standard Arithmetic Coding Technique (ACT) due to their frequencies and probabilities. Subtracting successive images contains two major types of values, zeros when subtracting similar areas, and significant values when subtracting different-color areas. In some cases, insignificant differences are noticed, where they can be justified by imaging errors. Such values are ignored and handled as zeros. After accomplishing the compression, Mean Normalization equation is used to shrink the number of bits required bits to represent these numbers using only 4 bits each. Then, each two successive 4-bits values are combined together to form a single by, which shrinks number of bytes into the half and doubles the CP ratio. Applying RLE and ACT is mandatory together due to their order, where they adopted due to the nature of data in each stage. Selecting sub-ROI yielded better results than the whole ROI or the total image area. The best number of trivial differences to be ignored is (2). Generally, the proposed compression scheme yielded superior results benchmarking State of Art literatures.

For future works, proposed scheme can be applied on other types of medical images such MRI or others. The concept of subtraction can be also used to be applied on successive frames of video files.

6. Acknowledgment

The authors would like to thank Middle Technical University (www.mtu.edu.iq) Baghdad, Iraq and Multimedia University, Kuala Lumpur, Malaysia (www.mmu.edu.my) for their support.

References

[1] Alkawaz M., Mydin M., and Johar M., "X-Ray, MRI and CT scan Medical Image Compression using Huffman Coding," *in Proceedings of the IEEE Symposium on Industrial Electronics and Applications*, Langkawi Island, pp. 1-6, 2022. 10.1109/ISIEA54517.2022.9873664

[2] Barman D., Hasnat A., and Barman B., "A Quantization Based Codebook Formation Method of Vector Quantization Algorithm to Improve the Compression Ratio While Preserving the Visual Quality of the Decompressed Image," *Multidimensional Systems and Signal Processing*, vol. 34, no. 1, pp. 127-145, 2023. https://doi.org/10.1007/s11045-022-00856-6

[3] Boopathiraja S. and Kalavathi P., "A Near Lossless Three-Dimensional Medical Image Compression Technique Using 3D-Discrete Wavelet Transform," *International Journal of Biomedical Engineering and Technology*, vol. 35, no. 3, pp. 191-206, 2021.

[4] Borrelli S., *Morphodynamic Imaging in Achalasia*, CRC Press, 2023. https://www.taylorfrancis.com/chapters/edit/10.1201/9781003320302-6/fluoroscopy-dynamic-barium-swallow-simona-borrelli

[5] Cazañas-Gordón A. and Parra-Mora E., "Digital compression in medical images," *Latin-American Journal of Computing*, vol. 9, no. 1, pp. 60-71, 2022. https://doi.org/10.5281/zenodo.5816321

[6] Chen J., Bai G., Liang S., and Li Z., "Automatic Image Cropping: A Computational Complexity Study," *in Proceedings of the IEEE conference on computer vision and pattern recognition*, Las Vegas, pp. 507-515, 2016. 10.1109/CVPR.2016.61

[7] Cole E., Park S., Kim S., Kang K., Valikodath N., Al-Khaled T., Montero-Mendoza C., and et al., "Variability in Plus Disease Diagnosis Using Single and Serial Images," *Ophthalmology Retina*, vol. 6, no. 12, pp. 1122-1129, 2022. DOI: 10.1016/j.oret.2022.05.024

[8] Dai L., Johar M., and Alkawaz M., "Review of Semi-Supervised Medical Image Segmentation based on the U-Net," *Academic Journal of Science and Technology*, vol. 11, no. 1, pp. 147-154, 2024. DOI: https://doi.org/10.54097/gmhkht38

[9] Daniel E., Lee R., and Williams J., "The reliability of Video Fluoroscopy, Ultrasound Imaging, Magnetic Resonance Imaging and Radiography for Measurements of Lumbar Spine Segmental Range of Motion in-Vivo: A Review, *Journal of Back and Musculoskeletal Rehabilitation*, vol. 36, no. 1, pp. 117-135, 2023. DOI: 10.3233/BMR-210285

[10] Dhar S., Nativ-Zeltzer N., Starmer H., Morimoto, L. Evangelista L., O'Rourke A., et al. "The

American Broncho-Esophagological Association Position Statement on Swallowing Fluoroscopy," *The Laryngoscope*, vol. 133, no. 2, pp. 255-268, 2023. DOI: 10.1002/lary.30177

[11] Estrela V., Deshpande A., Lopes R., Yin S., Andreopoulos N., Terziev A., and Laghari A., *In Intelligent Healthcare Systems*, CRC Press, 2023. DOI:10.1201/9781003196822-12

[12] Fadhil M., Naji M., and Salman G., "Transceiver Error Reduction by Design Prototype System Based on Neural Network Analysis Method," *Indonesian Journal of Electrical Engineering and Computer Science*, vol. 18, no. 3, pp. 1244-1251, 2020. DOI: 10.11591/ijeecs.v18.i3.pp1244-1251

[13] Fajar A., Sarno R., Fatichah C., and Fahmi A., "Reconstructing and Resizing 3D Images from DICOM Files," *Journal of King Saud University-Computer and Information Sciences*, vol. 34, no. 6, pp. 3517-3526, 2022. https://doi.org/10.1016/j.jksuci.2020.12.004

[14] Helliwell K., Hughes V., Bennion C., and Manning-Stanley A., "The Use of Videofluoroscopy (VFS) and Fibreoptic Endoscopic Evaluation of Swallowing (FEES) in The Investigation of Oropharyngeal Dysphagia in Stroke Patients: A Narrative Review," *Radiography*, vol. 29, no. 2, pp. 284-290, 2023. DOI: 10.1016/j.radi.2022.12.007

[15] Kadhim D., Mohamed F., Sakran A., Adnan M., and Salman G., "Early Diagnosis of Alzheimer's Disease Using Convolutional Neural Network-Based MRI," *Malaysian Journal of Fundamental and Applied Sciences*, vol. 19, no. 3, pp. 362-368, 2023.

[16] Keil H. and Trapp O., Fluoroscopic Imaging: New Advances, *Injury*, vol. 53, pp. S8-S15, 2022. DOI: 10.1016/j.injury.2022.05.035

[17] Li Z., Ramos, A., Li Z., Osborn M., Zaid W., Li, X., and Xu J., "Nearly-Lossless-To-Lossy Medical Image Compression by the Optimized JPEGXT and JPEG Algorithms through the Anatomical Regions of Interest," *Biomedical Signal Processing and Control*, vol. 83, pp. 104711, 2023. https://doi.org/10.1016/j.bspc.2023.104711

[18] Lim K., Yeo I., Ng S., Pan W., and Lee N., "The Machine-Vision Image Guided Surgery System Reduces Fluoroscopy Time, Ionizing Radiation and Intraoperative Blood Loss in Posterior Spinal Fusion for Scoliosis," *European Spine Journal*, vol. 32, no. 11, pp. 3987-3995, 2023. DOI: 10.1007/s00586-023-07848-5

[19] Mackenzie A., Lewis E., and Loveland J., "Successes and Challenges in Extracting Information from DICOM Image Databases for Audit and Research," *The British Journal of Radiology*, vol. 96, no. 1151, pp. 20230104, 2023. DOI: 10.1259/bjr.20230104.

[20] Majumdar P., Mitra S., Kumar Das S., and Majumdar P., *Human-Assisted Intelligent Computing: Modeling, Simulations and Applications*, 2023. DOI:10.1088/978-0-7503-4801-0ch15

[21] Mantri M., Taran S., and Sunder G., "DICOM Integration Libraries for Medical Image Interoperability: A Technical Review," *IEEE Reviews in Biomedical Engineering*, vol. 15, pp. 247-259, 2020. DOI: 10.1109/RBME.2020.3042642

[22] Mentzer F., Toderici G., Tschannen M., and Agustsson E., "High-Fidelity Generative Image Compression," *in Proceedings of the 34th Conference on Neural Information Processing Systems*, Vancouver, pp. 11913-11924, 2020.

[23] Merchant F. and Castleman K., *Microscope Image Processing*, Academic Press, 2022. https://www.sciencedirect.com/book/edited-volume/9780128210499/microscope-image-processing

[24] Nagoor O., Whittle J., Deng J., Mora B., and Jones M., "Lossless Compression for Volumetric Medical Images Using Deep Neural Network with Local Sampling," *in Proceedings of the IEEE International Conference on Image Processing*, Abu Dhabi, pp. 2815-2819, 2020. DOI: 10.1109/ICIP40778.2020.9191031

[25] Narayanaperumal M. and Ramraj R., "VLSI Implementations of Compressive Image Acquisition using Block Based Compression Algorithm," *The International Arab Journal of Information Technology*, vol. 12, no. 4, pp. 333-339, 2015.

[26] Pervan B., Tomic S., Ivandic H., and Knezovic J., MIDOM-A DICOM-Based Medical Image Communication System," *Applied Sciences*, vol. 13, no. 10, pp. 6075, 2023. https://doi.org/10.3390/app13106075

[27] Rani S., Glorindal G., and Herman I., "Medical Image Compression Using DCT with Entropy Encoding and Huffman on MRI Brain Images," *Asian Journal of Applied Science and Technology*, vol. 6, no. 2, pp. 16-25, 2022. https://ds.dmiseu.org/handle/123456789/91

[28] Rutherford M., Mun S., Levine B., Bennett W., Smith K., Farmer P., et al., "A DICOM dataset for evaluation of medical image de-identification," *Scientific Data*, vol. 8, no. 1, pp. 183, 2021. https://doi.org/10.6084/m9.figshare.14802774

[29] Salman S., Kadhim I., and Al-Badri A., "Image-Based Face Recognition Techniques Used in Disease Detection Approaches: A Survey," *Journal of Techniques*, vol. 6, no.1, pp. 33-44, 2024. DOI:10.51173/jt.v6i1.1966

[30] Shalom N., Gong G., and Auster M., "Fluoroscopy: An Essential Diagnostic Modality

in The Age of High-Resolution Cross-Sectional Imaging," *World Journal of Radiology*, vol. 12, no. 10, pp. 213-230, 2020. DOI: 10.4329/wjr.v12.i10.213

[31] Shyamala N. and Geetha S., "Improved Integer Wavelet Transform (IIWT) Based Medical Image Compression Method," *International Journal on Technical and Physical Problems of Engineering*, vol. 51, pp. 339-346, 2022.

[32] Singh D. and Singh B., "Investigating the Impact of Data Normalization on Classification performance," *Applied Soft Computing*, vol. 97, pp. 105524, 2020. https://doi.org/10.1016/j.asoc.2019.105524

[33] Singh U. and Kumar M., "A Review: Compression on Medical Images," *International Journal of Engineering and Technical Research*, vol. 11, no. 4, pp. 103-109, 2022.

[34] Siregar K., "Digital Image Compression Using Run Length Encoding Method," *Bios: Jurnal Informatika dan Sains*, vol.1, no. (01), pp. 20-24, 2023.

[35] Tong D., Nguyen T., Uyen B., Ngan L., Khanh L., and Tinh P., "Realistic Mathematics Education's Effect on Students' Performance and Attitudes: A Case of Ellipse Topics Learning," *European Journal of Educational Research*, vol. 11, no. 1, pp. 403-421, 2022. DOI: 10.12973/eu-jer.11.1.403

[36] Vijayan S. and Subramani M., "Unsupervised Convolutional Autoencoder Framework for Multimodal Medical Image Fusion in Brain Tumour Diagnosis," *The International Arab Journal of Information Technology*, vol. 22, no. 5, pp. 972-985, 2025. https://doi.org/10.34028/iajit/22/5/11

[37] Viswanthan P., and Palanisamy K., "Subband Thresholding for Near-Lossless Medical Image Compression," *International Journal of Computing and Digital Systems*, vol. 14, no. 1, pp. 63-72, 2023. DOI: 10.12785/ijcds/140106

[38] Yousif R. and Salman N., "Image Compression Based on Arithmetic Coding Algorithm," *Iraqi Journal of Science*, vol. 62, no. 1, pp. 329-334, 2021. DOI: https://doi.org/10.24996/ijs.2021.62.1.31

[39] Zafar S., Iftekhar N., Yadav A., Ahilan A., Kumar S., and Jeyam A., "An IoT Method for Telemedicine: Lossless Medical Image Compression Using Local Adaptive Blocks," *IEEE Sensors Journal*, vol. 22, no. 15, pp. 15345-15352, 2022. 10.1109/JSEN.2022.3184423

[40] Zhao N., MacDonald B., Pietrowski J., Laus J., Evangelista L., Joseph I., et al., "Clinician Accuracy in Identifying Essential Laryngeal Landmarks on Swallowing Fluoroscopy," *Laryngoscope Investigative Otolaryngology*, vol. 8, no. 5, pp. 1265-1271, 2023. DOI: 10.1002/lio2.1127

Ghalib Salman was born in Baghdad in 1969, and get his Bsc. degree at Baghdad University/College of Administration/ Department of Statistics. His master degree was in computer science/ image Steganography at University of Technology- Baghdad, and his Ph.D. was accomplished in University Technology of Malaysia in computer science (image processing). His career contained about 32 years in the field of scientific research and academic teaching experiences. He published about 20 articles in the field of Image processing. His current job is a lecturer in the Department of Medical Devices Engineering Electrical Engineering Technical College, Middle Technical University, Baghdad, Iraq.

Arif Arif was born in Baghdad in 1970, he was obtained a bachelor's degree from Al-Mustansiriya University/College of Science, Department of Mathematics. The master's degree in computer science image processing from the University of Technology. The Ph.D. in computer science image processing from Multimedia University (MMU) Cyberjaya Malaysia. He has nearly 25 years teaching experience in the Department of Computer Science. He is currently work as a lecturer in the Department of Computer Systems Techniques, Institute of Administration Al Russaffa, Middle Technical University, Baghdad, Iraq. He published more than 15 articles in international and national journals and conferences.

Sarina Mansor is an Associate Professor in the Faculty of Applied Intelligence and Engineering (FAIE) at Multimedia University (MMU) Malaysia. She is currently the Program Coordinator of B.Eng. (Hons) Electronics Majoring in Computer. She received her B.Eng (Hons) Electronic and Electrical from University of College London in 1998 and M.EngSc degree from Multimedia University in 2002. She completed her DPhil in Engineering Science from University of Oxford (UK) in 2009. Her research interests are Signal and Image Analysis, Medical Imaging, Computer Vision, Machine Learning and Internet of Things. She can be